Journal of
NANOSTRUCTURES

JNS
NANOSTRUCTURES
JNS.kashanu.ac.ir

Synthesis and Characterization of Nano-Sized Hexagonal and Spherical Nanoparticles of Zinc Oxide

M. A. Moghri Moazzen [a,*], S. M. Borghei [b], F. Taleshi [c]

[a] *Young Researchers Club, Karaj Branch, Islamic Azad University, Karaj, Iran.*

[b] *Department of Physics, Karaj Branch, Islamic Azad University, Karaj, Iran.*

[c] *Department of Applied Sciences, Qaemshahr Branch, Islamic Azad University, Qaemshahr, Iran.*

*Corresponding author:
E-mail address*:*
m_moghri_moazzen@yahoo.com
Phone: +98 9119095028
Fax: +982634418156

Abstract

ZnO plays an important role in many semiconductors technological aspects. Here, direct precipitation method was employed for the synthesis of nano-sized hexagonal ZnO particles, which is based on chemical reactions between raw materials used in the experiment. ZnO nanoparticles were synthesized by calcinations of the ZnO precursor precipitates at 250 ˚C for 3hours. The particle size and structure of the products have been confirmed by XRD. The FT-IR study confirms the presence of functional groups. Also, the morphology and size distribution of ZnO nanoparticles was analyzed by TEM images. The optical properties were investigated by UV–Visible spectroscopy. The XRD results show that the size of the prepared nanoparticles is in the range of 20–40 nm, which this value is in good agreement with the TEM results. The FT-IR spectrum clearly indicates the formation of an interfacial chemical bond between Zn and O. Also the UV absorption depends on the particles size and morphology, so the optical properties enhances with decreasing nanoparticles size. Moreover the direct precipitation technique is a feasible method for production of ZnO nanopowders.

1. Introduction

In recent years, the synthesis and functionalism of nanostructures have attracted vast and persistent interest because of their significant potential application. The ZnO is known to be a wide band-gap (3.37 eV) with a high exciton binding energy (60 meV) and exhibit the most sheeny and numerous configuration of nanostructure that one material can form. Also, ZnO as an important semiconducting material has a wide range of

applications in gas sensors, chemical absorbent, nanogenerators, electrical and optical devices, electrostatic dissipative coatings, and advanced ceramics [1].

The properties of the ZnO closely depend on the nanostructures of the materials, including crystal size, orientation and morphology, aspect ratio and even crystalline density [2]. The high surface area and morphology also have an important role in many applications. A variety of different morphologies of ZnO nanostructures including wires, rods, spheres, flowers, combs, balls have been synthesized to date [3-7]. Therefore, there are various physical and chemical methods for the product of different ZnO nanostructures with controlled crystalline morphology, orientation and surface architectures. The physical methods such as DC magnetron sputtering, RF magnetron sputtering, vapour phase deposition, metal-organic vapor-phase epitaxy (MOVPE), and pulsed laser deposition (PLD) [8-12]. Further, the chemical methods including sol-gel, micro-emulsion, hydrothermal, self-assembly, homogenous, microwave assisted hydrothermal and direct precipitation [13-16] have been reported for synthesis of ZnO nanostructures. In precipitation methods, the zinc sources are generally zinc nitrate and zinc acetate.

In this study, we have investigated the role of different concentration ratios of reactants for synthesis of ZnO nanoparticles via direct precipitation method (DPM). Here, ZnO nanoparticles were prepared by precipitation from zinc acetate dehydrate and sodium hydroxide. The ratio of concentration of precursor was varied from 1:1 to 1:4 (zinc acetate dehydrate: Sodium hydroxide). This method exhibits several advantages like low equipment and low cast, large scale production, low-temperature process and no

catalyst assistant. ZnO nanoparticles were obtained and their size, morphology, structure, and optical properties were studied.

2. Experimental procedure

All the chemicals used in this study were of analytical grade and used without further purification. First, zinc acetate dehydrate (Merck, 99%) and sodium hydroxide (Merck, 99%) was dissolved in distilled deionized water to form liquid mediums with necessary concentrations. Zinc acetate dehydrate solution was slowly added drop wise into sodium hydroxide solution under vigorous stirring at room temperature and formed a transparent white solution. In this way, for earning the optimal condition, different concentration ratios of aqueous solutions of zinc acetate dehydrate to the sodium hydroxide were prepared. The ratios of concentration were varied from 1:1 to 1:4 (zinc acetate dehydrate: sodium hydroxide). These solutions were slowly reacted to produce the precipitates of ZnO particles. In the next step, the precipitates derived after the reaction between zinc acetate dehydrate and sodium hydroxide solutions were collected by filtration and rinsed three times with distilled deionized water and ethanol. Afterwards, the washed precipitates were dried in an electric oven at 100°C for 5h until the precursors of ZnO to be formed. At the final step, the precursors were calcinated at a temperature of 250°C for 3h to obtain the ZnO nanopowder. The 1:1 concentration ratio (zinc acetate dehydrate: sodium hydroxide) was optimum sample.

The crystallinity and crystal phases of the nanoparticles were analyzed by the X-ray diffraction (MMA, GBC) spectroscopy with Cu Ka radiation (λ= 1.54 A °) in the range of 20–80° by a step size of 0.05° per second. The structural and morphological investigation was carried out by

transmission electron microscopy (Philips, CM10). The Fourier transform infrared absorption (FT-IR) spectroscopy was carried out at room temperature by the FT-IR spectrophotometer. For this spectroscopy, a pellet of the powder was prepared with KBr. The optical properties of the samples were studied by the UV–visible (UV–Vis) absorption double beam spectrophotometer with a deuterium and tungsten iodine lamp.

3. Results and discussion

The XRD patterns of ZnO nanoparticles are showed in Fig. 1. All peaks can be well indexed to the hexagonal phase of ZnO with a wurtzite structure (JCPDS 36-1451). No peaks from other phase of ZnO and impurities are observed, confirming that high-purity ZnO nanoparticles be obtained. The strong and narrow diffraction peaks indicate that the nanoparticles have a good crystallinity and size.
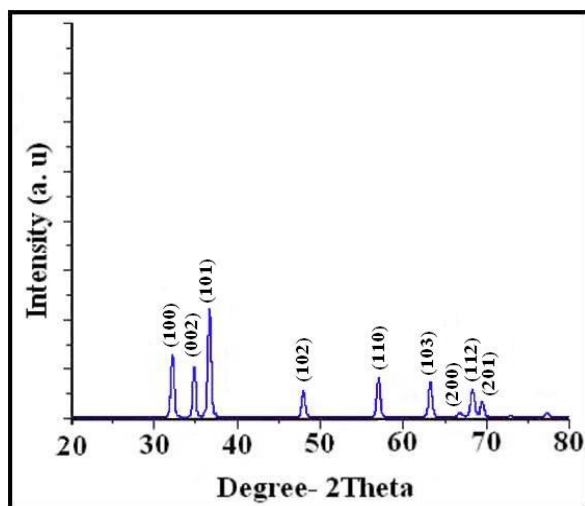

Fig. 1. XRD patterns of ZnO nanoparticles with 1:1 concentration ratio.

The ZnO crystallite sizes are calculated using Debye-Scherrer's formula [1],

$$D = (0.89\,\lambda)/(\beta \cos \theta) \qquad (1)$$

Therein, λ is the wavelength of the Cu kα radiation (1.54 A˚), β is the full width at half maximum of the peak, and θ is the Bragg's angle obtained from the 2θ value corresponding to the maximum intensity peak in XRD pattern. Clearly, an increase in concentration ratios brings about a corresponding increase on crystallite size and leading to sharper diffraction peaks and the results are given in Table 1. We are notice that the applicability of Scherrer's formula is restricted to small particles (usually smaller than 100 nm) and the above observed that the average size of the nanoparticles varied from 20 to 36 nm.

Table 1. Crystallite sizes of the ZnO nanoparticles with different concentration ratios.

Sample	Con. ratio [wt%]	FWHM (deg)	Particle Size (nm)
a	1:1	0.44	20
b	1:2	0.30	27
c	1:3	0.27	30
d	1:4	0.23	36

In order to study the mechanism of the functionalization process, the FT-IR spectra of the obtained optimum ZnO precursor dried at 100°C for 5 h were examined. Fig. 2 shows the FT-IR spectra of the sample, the absorption peaks at 3250 cm^{-1} and 3400 cm^{-1} attributed to hydroxyl (OH) groups, The FT-IR absorption band at 410 cm^{-1} was the characteristic absorb peak of ZnO. Also, peaks at 1400, 1560, 2900 and 2980 cm^{-1} are attributed to the asymmetric and symmetric stretching vibrations CH_2 and CH_3 groups. These results prove that the C_2H_5OH molecule remained in a strong chemical adsorption on the precursor surface and by thermal decomposition process will be removed.
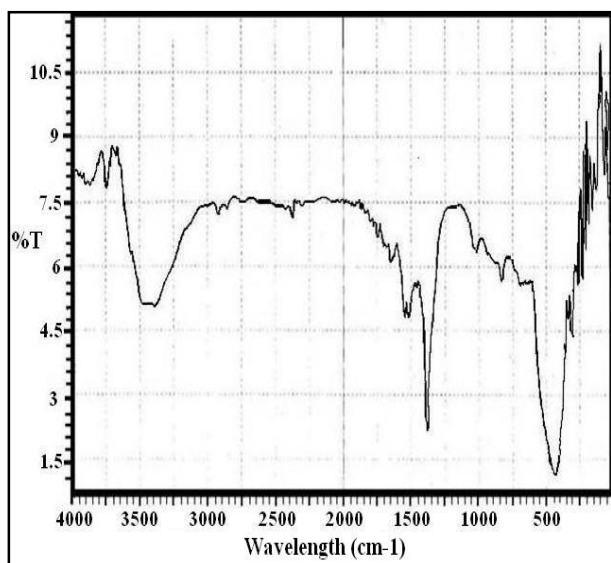
Fig. 2. FT-IR spectrum of the ZnO precursor dried at 100 °C for 5 h.

Fig. 3 shows the FT-IR spectrum of ZnO nanoparticles calcinated at 250 for 3 h. As can be seen, there aren't any of the previous peaks after calcinations. Therefore, during the thermal decomposition precursor process, C_2H_5OH molecule disported of the precursor surface and we consider that the grains are high-purity of ZnO nanoparticles.
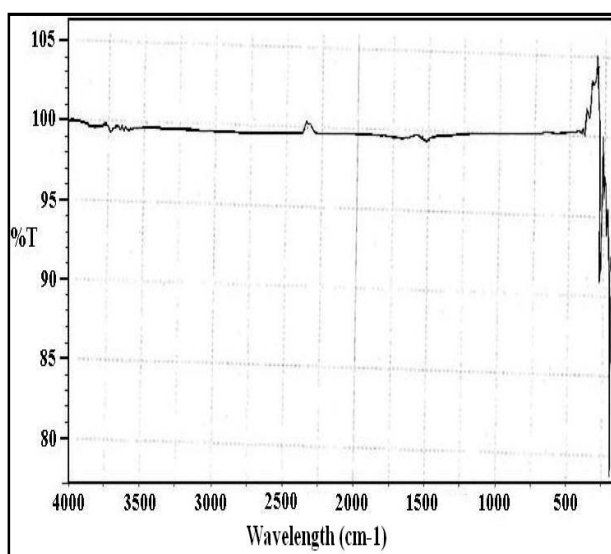
In the process of ZnO nanoparticles preparation by direct precipitation method, concentration ratios of reactants have a great effect on the size distribution and dispersion of ZnO. The actual size of optimum ZnO nanoparticles, which can be seen from the TEM images shown in Fig. 4, was 18 nm. Also, observed ZnO nanoparticles are approximately both spherical and hexagonal. We know that, at best condition, the precision of crystallite size analysis by Debye-Scherer is of the order of ±10٪ [17]. However, the nanoparticles size estimated by X-ray diffraction, which identifies the underlying lattice planes, is 20nm. This value of nanoparticles size is in good agreement with the TEM result with an acceptable precision limit. Thus, our samples have a high surface area which is appropriate for applications in advanced technologies.
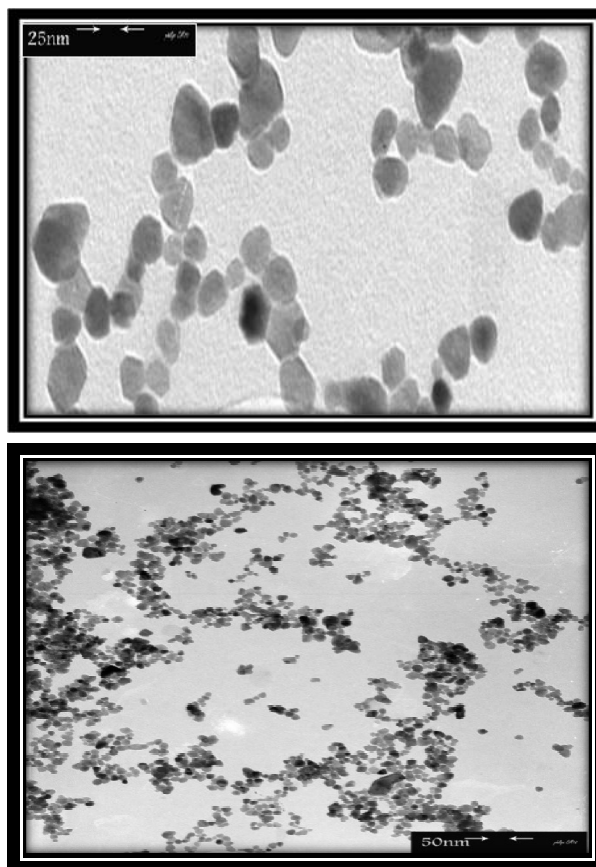

Fig. 4. TEM images of ZnO nanoparticles.

Fig. 3. FT-IR spectrum of the ZnO nanoparticles calcinated at 250°C for 3 h.

The UV–Vis absorption of the ZnO nanoparticles is related to their size. As we know that the interface and surface play a key role in the light absorption of materials [18]. The UV–Vis spectrum of the ZnO nanoparticles was observed by dispersing the powder in deionized water. Fig. 5 shows the UV–Vis spectrum of ZnO nanoparticles measured at room temperature. A broad band can be seen at 317 nm (3.30 eV), which is very close to the band gap of ZnO 1s–1s electron transition (3.37 eV) [18].
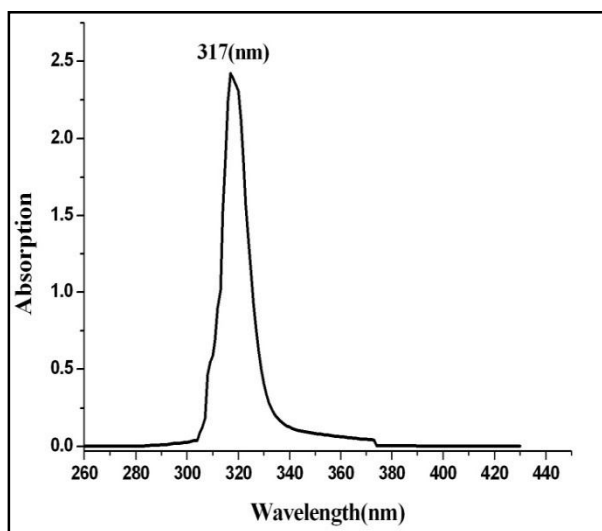

Fig. 5. UV-Vis spectrum of the nano-sized ZnO powders.

4. Conclusion

ZnO nanoparticles were synthesized with different concentration ratios of zinc acetate dehydrate to Sodium hydroxide by direct precipitation method at room temperature. XRD results show formation of hexagonal wurtzite ZnO structure with high crystallinity. TEM revealed the size distribution of nanoparticles. The actual average size of optimum ZnO nanoparticles was 18 nm, which the estimated sizes given by XRD and TEM are in good agreement. Observed ZnO nanoparticles were approximately both spherical and hexagonal.

Optical properties of the ZnO nanoparticles depended on the size of nanoparticles. The UV light absorbance of the ZnO nanoparticles increases generally with decreasing particles. So the optical properties get better with increasing ratio of surface to volume in ZnO nanoparticles. Results reported herein provide a facile and with desired properties.

References

[1] U. Ozgur, Y. I. Alivov, J. Appl. Phys. 98 (2005) 41301.
[2] C. Wu, X. Qiao, J. Chen, H. Wang, F. Tan, S. Li, Materials Letters. 60 (2006) 1828–1832.
[3] Z. L. Wang, J. H. Song, Science. 14 (2006) 242-246.
[4] Z. Zhang, H. Yu, X. Shao, M. Han, Chem. Eur. J. 11 (2005) 3149-3154.
[5] J. Zhang, S. Wang, Y. Wang, M. Xu, H. Xia, S. Zhang, W. Huang, X. Guo, S. Wu, Sensors and Actuators B: Chemical. 3 (2009) 14.
[6] Y. J. Kim, J. Yoo, B. H. Kwon, Y. J. Hong, C. H. Lee, G. C. Yi, Nanotechnology. 19 (2008) 315202.
[7] J. X. Wang, X. W. Sun, A. Wei, Y. Lei, X. P. Cai, C. M. Li, Z. L. Applied Physics Letters. 88 (2006) 233106.
[8] G. Kiriakidis, M. Suchea, S. Christoulakis, P. Horvath, T. Kitsopoulos, J. Stoemenos. Thin Solid Films. 515 (2007) 8577–8581.

[9] N. Hongsith, S. Choopun, S. Tanunchai, T. Chairuangsri, P. Mangkorntong, N. Mangkorntong," Chiang Mai J. Sci. 32(3) (2005) 417-420.

[10] V. K. Pillai, N. S. Ramgir, D. J. Late, A. B. Bhise, I. S. Mulla, M. A. More, D. S. Joag. Nanotechnology, 17 (2006) 2730–2735.

[11] W. I. Park, D. H. Kim, S. W. Jung, G. C. Yi, Appl. Phys. Lett. 80 (2002) 4232.

[12] R. S. Aimsha, R. Manoj, P. M. Aneesh, M. K. Jayaraj, Curr. Appl. Phys. 10 (2010) 693.

[13] G. Hohenberger, G. Tomandi J. Mater. Res. 7 (1992) 546-548.

[14] B. Liu, H. C. Zeng, J. Am. Chem. Soc. 125 (2003) 4430-4431.

[15] J. H. Kim, W. C. Choi, H. Y. Kim, Y. Kang, Y. K. Park, Powder Technol. 153 (2005) 166-175.

[16] J. M. Wang, L.Gao, Inorg. Chem. Commun. 6 (2003) 877-881.

[17] B. D. Eullity, Wesley Publishing company Inc, USA, 1978.

[18] P. T. Hsieh, Y. C. Chen, Journal of the European ceramic Society. 27 (2007) 3815-3818.